

A possible scenario for the fragile-to-strong dynamic crossover predicted by the extended mode-coupling theory for glass transition

This article has been downloaded from IOPscience. Please scroll down to see the full text article.

2009 J. Phys.: Condens. Matter 21 504101

(<http://iopscience.iop.org/0953-8984/21/50/504101>)

View [the table of contents for this issue](#), or go to the [journal homepage](#) for more

Download details:

IP Address: 129.252.86.83

The article was downloaded on 30/05/2010 at 06:23

Please note that [terms and conditions apply](#).

A possible scenario for the fragile-to-strong dynamic crossover predicted by the extended mode-coupling theory for glass transition

S-H Chong¹, S-H Chen² and F Mallamace³

¹ Institute for Molecular Science, Okazaki 444-8585, Japan

² Department of Nuclear Science and Engineering, Massachusetts Institute of Technology, Cambridge, MA 02139, USA

³ Dipartimento di Fisica, Università di Messina and IRCCS Neurolesi 'Bonino-Pulejo', I-98166 Messina, Italy

E-mail: chong@ims.ac.jp

Received 17 April 2009

Published 23 November 2009

Online at stacks.iop.org/JPhysCM/21/504101

Abstract

It is argued that the extended mode-coupling theory for glass transition predicts a dynamic crossover in the α -relaxation time and in the self-diffusion constant as a general implication of the structure of its equations of motion. This crossover occurs near the critical temperature T_c of the idealized version of the theory, and is caused by the change in the dynamics from the one determined by the cage effect to that dominated by hopping processes. When combined with a model for the hopping kernel deduced from the dynamical theory for diffusion-jump processes, the dynamic crossover can be identified as the fragile-to-strong crossover (FSC) in which the α -relaxation time and the self-diffusion constant cross over from a non-Arrhenius to an Arrhenius behavior. Since the present theory does not resort to the existence of the so-called Widom line, to which the FSC in confined water has been attributed, it provides a possible explanation of the FSC observed in a variety of glass-forming systems in which the existence of the Widom line is unlikely. In addition, the present theory predicts that the Stokes-Einstein relation (SER) breaks down in different ways on the fragile and strong sides of the FSC, in agreement with the experimental observation in confined water. It is also demonstrated that the violation of the SER in both the fragile and strong regions can be fitted reasonably well by a single fractional relation with an empirical exponent of 0.85.

(Some figures in this article are in colour only in the electronic version)

1. Introduction

A fragile-to-strong dynamic crossover (FSC) phenomenon has been observed in confined water in which the α -relaxation time [1, 2] and the inverse of the self-diffusion constant [3] cross over from a non-Arrhenius to an Arrhenius behavior. The FSC is considered to be caused by the hypothesized existence of the liquid-liquid critical point in water [4, 5]: it is attributed to crossing of the Widom line (the line of maximum correlation length) emanating from the liquid-liquid critical point [6, 7].

On the other hand, it has been recognized that the viscosity data on various glass-forming liquids exhibit an FSC-like feature at a crossover temperature T_0 : while the temperature dependence of the viscosity of many glass-forming liquids can be well described by a power law for $T > T_0$, it smoothly crosses over to approximately an Arrhenius behavior for $T < T_0$ [8–10]. Recent measurements of diffusion constants in bulk glass-forming alloys also display the crossover from a non-Arrhenius to an Arrhenius behavior [11, 12]. Thus, the FSC seems a common, or at least an unexceptional, phenomenon in glass-forming systems, which is in contrast to

a traditional view that a glass-forming liquid can be classified either as fragile or strong [13]. Since it is unlikely that the Widom line exists for most glass formers, there should be some other mechanism which is responsible for the FSC. In this paper, a possible scenario for the FSC is discussed based on the extended mode-coupling theory (MCT) for glass transition [14, 15], which does not resort to the presence of the Widom line. This is motivated by the observation that the mentioned crossover temperature T_0 , which is typically located about 20% above the glass transition temperature T_g , is considered to coincide with the critical temperature T_c of the idealized version of MCT [10, 11].

This paper is organized as follows. In section 2, we argue that the extended MCT predicts a dynamic crossover in the α -relaxation time and in the self-diffusion constant at $T \approx T_c$ as the dynamics changes from the one determined by the cage effect to that dominated by hopping processes. Numerical results are presented in section 3 to demonstrate the theoretical prediction. The paper is summarized in section 4 with some concluding remarks.

2. Theory

In this section, we argue that the extended MCT predicts a dynamic crossover in the α -relaxation time and in the self-diffusion constant and that this crossover occurs near the critical temperature T_c of the idealized version of the theory. We start from surveying basic features of the idealized [16] and extended [14, 15] MCT. A system of N spherical particles of mass m distributed with the average number density ρ shall be considered. Structural changes as a function of time t are characterized by coherent density correlators $\phi_q(t) = \langle \rho_q^* e^{i\mathcal{L}t} \rho_q \rangle / N S_q$ which are normalized to unity at $t = 0$. Here $\rho_{\vec{q}} = \sum_i \exp(i\vec{q} \cdot \vec{r}_i)$, with \vec{r}_i referring to the i th particle's position, denotes density fluctuations for wavevector \vec{q} ; \mathcal{L} the Liouville operator; $\langle \dots \rangle$ the canonical averaging for temperature T ; $S_q = \langle \rho_q^* \rho_q \rangle / N$ the static structure factor; and $q = |\vec{q}|$.

The idealized-MCT equations consist of the exact Zwanzig–Mori equation:

$$\partial_t^2 \phi_q(t) + \Omega_q^2 \phi_q(t) + \Omega_q^2 \int_0^t dt' m_q(t-t') \partial_{t'} \phi_q(t') = 0 \quad (1)$$

in which $\Omega_q^2 = q^2 k_B T / m S_q$ with Boltzmann's constant k_B , and the following idealized-MCT expression for the memory kernel to be denoted as $m_q^{\text{id}}(t)$:

$$m_q^{\text{id}}(t) = \int d\vec{k} V(\vec{q}; \vec{k}, \vec{p}) \phi_k(t) \phi_p(t). \quad (2)$$

Here $V(\vec{q}; \vec{k}, \vec{p}) = \rho S_q S_k S_p [(\vec{q} \cdot \vec{k}) c_k + (\vec{q} \cdot \vec{p}) c_p]^2 / [2(2\pi)^3 q^4]$, $\vec{p} = \vec{q} - \vec{k}$ and $c_q = (1 - 1/S_q) / \rho$. The idealized-MCT equations (1) and (2) exhibit a bifurcation for $\phi_q(t \rightarrow \infty) = f_q$ —also referred to as the nonergodic transition—at a critical temperature T_c [16]. For $T > T_c$, the correlator relaxes towards $f_q = 0$ as expected for ergodic liquid states. On the other hand, density fluctuations for $T \leq T_c$ arrest in a disordered solid, quantified by a Debye–Waller factor $f_q > 0$.

The extended-MCT equations also consist of the Zwanzig–Mori equation (1), but the memory kernel entering there has the following extended form:

$$m_q(z) = m_q^{\text{id}}(z) / [1 - \delta_q(z) m_q^{\text{id}}(z)] \quad (3)$$

with an additional kernel $\delta_q(z)$, called the hopping kernel, which takes into account the effect from hopping processes. Here we have introduced the Laplace transform with the convention $f(z) = i \int_0^\infty dt e^{izt} f(t)$ ($\text{Im } z > 0$). The extended memory kernel $m_q(z)$ in (3) thus deals with the interplay of two effects. Nonlinear interactions of density fluctuations, as described by the idealized memory kernel $m_q^{\text{id}}(z)$, lead to the cage effect with a trend to produce arrested states for $T \leq T_c$. On the other hand, the hopping processes, taken into account via the hopping kernel $\delta_q(z)$, lead to the α relaxation and restore ergodicity at all temperatures (see below). A model for the hopping kernel shall not be specified here (see section 3 for the model adopted in the present work) since our argument below does not depend on the specific model for $\delta_q(z)$.

It is more convenient for the following discussion to reformulate the extended-MCT equations in the form

$$\phi_q(z) = -1/[z + K_q(z)] \quad (4)$$

in terms of the Laplace form $K_q(z)$ of the longitudinal current correlator. Combining the Laplace transform of (1), $\phi_q(z) = -1/[z - \Omega_q^2/[z + \Omega_q^2 m_q(z)]]$, with (3), one finds [17]

$$K_q(z) = \delta_q(z) - \frac{\Omega_q^2 [1 + R_q^{(2)}(z)]}{z + [1 + R_q^{(1)}(z)] \Omega_q^2 m_q^{\text{id}}(z)}. \quad (5)$$

Here $R_q^{(1)}(z) = -z\delta_q(z)/\Omega_q^2$ and $R_q^{(2)}(z) = z\delta_q(z)[1 - \delta_q(z)m_q^{\text{id}}(z)]/\Omega_q^2$ are renormalization functions, which are unimportant in the low-frequency regime $z \rightarrow 0$ (or the long-time regime) of interest. Neglecting these terms, the function $K_q(z)$ gets the following transparent form:

$$K_q(z) = \delta_q(z) + K_q^{\text{id}}(z) \quad \text{with } K_q^{\text{id}}(z) = -\frac{\Omega_q^2}{z + \Omega_q^2 m_q^{\text{id}}(z)}. \quad (6)$$

Dropping $\delta_q(z)$, this equation reduces to the one of the idealized MCT, $K_q(z) = K_q^{\text{id}}(z)$: approaching the critical temperature T_c from above, $m_q^{\text{id}}(z)$ becomes larger due to the cage effect and the current correlator $K_q(z)$ vanishes at $T = T_c$, leading to the sharp nonergodic transition. In the presence of $\delta_q(z)$, on the other hand, the term $K_q^{\text{id}}(z)$ becomes unimportant when $m_q^{\text{id}}(z)$ becomes large and there holds $K_q(z) \approx \delta_q(z)$. The hopping kernel takes over and hinders the currents from vanishing, thereby preventing the density fluctuations from becoming arrested completely. Thus, there occurs a dynamics crossover at $T \approx T_c$ from the cage-effect-dominated regime, where $K_q(z) \approx K_q^{\text{id}}(z)$, to the hopping-dominated regime, in which $K_q(z) \approx \delta_q(z)$.

Let us see an implication of such a crossover for the α -relaxation time τ_q of the coherent density correlator $\phi_q(t)$, which can be estimated from $\tau_q \sim \int_0^\infty dt \phi_q(t)$, i.e. $i\tau_q \sim \phi_q(z \rightarrow 0)$. In view of (4), one understands that $K_q(z \rightarrow 0)$

is connected to τ_q via $K_q(z \rightarrow 0) \sim i/\tau_q$. Equation (6) then implies

$$1/\tau_q \approx 1/\tau_q^{\text{hop}} + 1/\tau_q^{\text{id}} \quad (7)$$

in which we have introduced τ_q^{hop} due to the hopping processes via $\delta_q(z \rightarrow 0) = i/\tau_q^{\text{hop}}$. Thus, the extended MCT predicts a dynamic crossover in the α -relaxation time τ_q at $T \approx T_c$ from $\tau_q \approx \tau_q^{\text{id}}$ to $\tau_q \approx \tau_q^{\text{hop}}$.

We next turn our attention to the tagged-particle dynamics. Of special interest here is the self-diffusion constant D , which is given by the integral $D = \int_0^\infty dt K^s(t)$ of the velocity autocorrelation function $K^s(t) = \langle \vec{v}_s(t) \cdot \vec{v}_s(0) \rangle / 3$ [18]. Hereafter, quantities referring to the tagged particle (labeled s) shall be marked with the superscript or subscript ‘ s ’ and $\vec{v}_s(t)$ denotes the velocity of the tagged particle at time t . The Zwanzig–Mori equation for the tagged-particle density correlator $\phi_q^s(t) = \langle \rho_q^{s*} e^{i\vec{L}t} \rho_q^s \rangle$ with $\rho_q^s = \exp(i\vec{q} \cdot \vec{r}_s)$ has the same form as (1) with ϕ_q , m_q and Ω_q^2 replaced by ϕ_q^s , m_q^s and $(\Omega_q^s)^2 = q^2 k_B T / m$, respectively; the idealized-MCT memory kernel corresponding to (2) is given by $m_q^{\text{sid}}(t) = \int d\vec{k} V^s(\vec{q}; \vec{k}, \vec{p}) \phi_k(t) \phi_p^s(t)$ with $V^s = \rho S_k [(i\vec{q} \cdot \vec{k})c_k]^2 / [(2\pi)^3 q^4]$ [19]; and the extended memory kernel is given by (3) with m_q , m_q^{id} and δ_q replaced by m_q^s , m_q^{id} and δ_q^s , respectively. The arrested part f_q^s of the correlator $\phi_q^s(t)$ in the idealized theory is referred to as the Lamb–Mössbauer factor.

Let us note that $K^s(t)$ and the mean-squared displacement, $\delta r^2(t) = \langle [\vec{r}_s(t) - \vec{r}_s(0)]^2 \rangle$, are related via $K^s(t) = (1/6) \partial_t^2 \delta r^2(t)$. Therefore, the extended-MCT equations for $K^s(t)$ can be deduced from those for $\delta r^2(t)$, which have been derived in [15] exploiting the small- q behavior of $\phi_q^s(t) = 1 - q^2 \delta r^2(t) / 6 + O(q^4)$ [18]. The resulting equations for $K^s(t)$ consist of the Zwanzig–Mori equation:

$$\partial_t K^s(t) + v^2 \int_0^t dt' m_s(t-t') K^s(t') = 0 \quad (8)$$

in which $v^2 = k_B T / m$, and the following expression for the memory kernel:

$$m^s(z) = m^{\text{id}}(z) / [1 - \delta^s(z) m^{\text{id}}(z)]. \quad (9)$$

Here $m^s(t) = \lim_{q \rightarrow 0} q^2 m_q^s(t)$ and $\delta^s(z) = \lim_{q \rightarrow 0} \delta_q^s(z) / q^2$. Combining the Laplace transform of (8), $K^s(z) = -v^2 / [z + v^2 m^s(z)]$, with (9), one finds

$$K^s(z) = \delta^s(z) - \frac{v^2 [1 + R^{s(2)}(z)]}{z + [1 + R^{s(1)}(z)] v^2 m^{\text{id}}(z)}. \quad (10)$$

Again, $R^{s(1)}(z) = -z \delta^s(z) / v^2$ and $R^{s(2)}(z) = z \delta^s(z) [1 - \delta^s(z) m^{\text{id}}(z)] / v^2$ are renormalization functions, which are unimportant in the low-frequency regime $z \rightarrow 0$. Neglecting these terms, there holds

$$K^s(z) = \delta^s(z) + K^{\text{id}}(z) \quad \text{with } K^{\text{id}}(z) = -\frac{v^2}{z + v^2 m^{\text{id}}(z)}. \quad (11)$$

Since $K^s(z \rightarrow 0) = iD$, this relation implies

$$D \approx D^{\text{hop}} + D^{\text{id}} \quad (12)$$

in which we have introduced D^{hop} via $\delta^s(z \rightarrow 0) = iD^{\text{hop}}$. Thus, the extended MCT predicts that the self-diffusion constant D also exhibits a dynamic crossover at $T \approx T_c$ from $D \approx D^{\text{id}}$ to D^{hop} .

3. Results and discussion

In the following, numerical results of the theory are presented for the Lennard-Jones (LJ) system in which particles interact via the potential $V(r) = 4\epsilon_{\text{LJ}} \{ (\sigma_{\text{LJ}}/r)^{12} - (\sigma_{\text{LJ}}/r)^6 \}$. Hereafter, all quantities are expressed in reduced units with the unit of length σ_{LJ} , the unit of energy ϵ_{LJ} (setting $k_B = 1$) and the unit of time $(m\sigma_{\text{LJ}}^2/\epsilon_{\text{LJ}})^{1/2}$. The static structure factor S_q , which is required for determining Ω_q^2 , $m_q^{\text{id}}(t)$ and $m_q^{\text{id}}(t)$, shall be evaluated within the Percus–Yevick approximation [18]. The critical temperature of the idealized MCT for this model is found to be $T_c = 1.637$ for the average number density $\rho = 1.093$ [20] to be considered in the present work.

As a model for the hopping kernel entering into the extended MCT, we shall adopt the one developed in [15]. In this model, the hopping processes are incorporated via the dynamical theory [21] originally formulated to describe diffusion–jump processes in crystals. The dynamical theory approach treats hopping as arising from vibrational fluctuations in the quasi-arrested state where particles are trapped inside their cages, and the resulting hopping rate w_{hop} under the isotropic Debye approximation is [15]

$$w_{\text{hop}} = \frac{1}{2\pi} \left(\frac{3}{5} \right)^{1/2} \omega_D \exp \left[-\frac{3m v_L^2}{2k_B T} \Delta^2 \right] \quad (13)$$

in terms of the sound velocity $v_L = \sqrt{k_B T / m S_0 (1 - f_0)}$ in the quasi-arrested state, which is renormalized by the Debye–Waller factor $f_0 = \lim_{q \rightarrow 0} f_q$ [20, 22]. $\omega_D = k_D v_L$ with $k_D = (6\pi^2 \rho)^{1/3}$ denotes the Debye frequency. Δ is a dimensionless measure of the critical size of the phonon-assisted fluctuation needed to cause a hopping and we set $\Delta^2 = 0.10$ in the present work which is estimated in [21] from migration properties of crystals. We notice that this value of Δ^2 is consistent with the Lindemann length [15]. The collective and tagged-particle hopping kernels are then given by

$$\delta_q(z) = \delta_q^s(z) / S_q, \quad \delta_q^s(z) = i w_{\text{hop}} N_c [1 - \sin(qa)/(qa)] / f_q^s. \quad (14)$$

Here N_c is the coordination number of the first shell surrounding a particle and a denotes the hopping distance which is assumed to be given by the average interparticle distance. (See [15] on how N_c and a can be evaluated based on the knowledge of the radial distribution function.)

Figure 1 shows the coherent density correlator $\phi_q(t)$ at the peak position $q = 7.3$ of the static structure factor for representative temperatures near T_c whose values are specified in the caption. The dashed curves refer to the idealized-MCT results, which exhibit the bifurcation of the long-time limit at $T = T_c$, i.e. $\phi_q(t \rightarrow \infty) = 0$ for $T > T_c$, whereas $\phi_q(t \rightarrow \infty) = f_q > 0$ for $T \leq T_c$ [16]. The solid curves denote the results from the extended MCT, according to which the density correlator eventually relaxes to zero even for

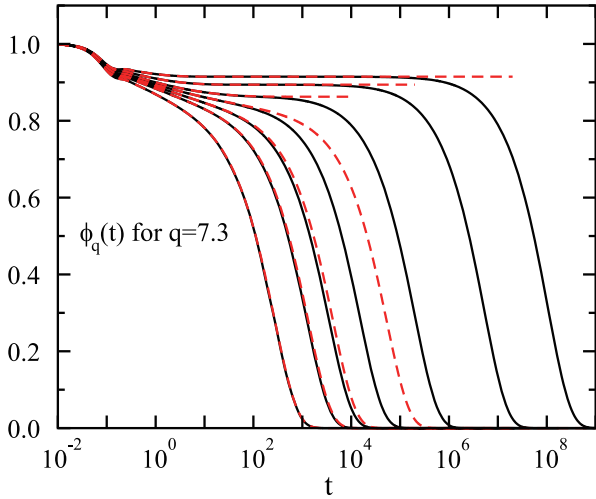


Figure 1. Coherent density correlator $\phi_q(t)$ at the peak position $q = 7.3$ of the static structure factor for temperatures $T = T_c(1 - \epsilon)$ with $T_c = 1.637$ and $\epsilon = -0.10, -0.05, -0.03, -0.01, +0.01, +0.05$ and $+0.10$ (from left to right). The solid curves denote the results from the extended MCT. The dashed curves refer to the results from the idealized MCT, which exhibit the bifurcation of the long-time limit at $T = T_c$, i.e., $\phi_q(t \rightarrow \infty) = 0$ for $T > T_c$ ($\epsilon < 0$), whereas $\phi_q(t \rightarrow \infty) = f_q > 0$ for $T \leq T_c$ ($\epsilon \geq 0$).

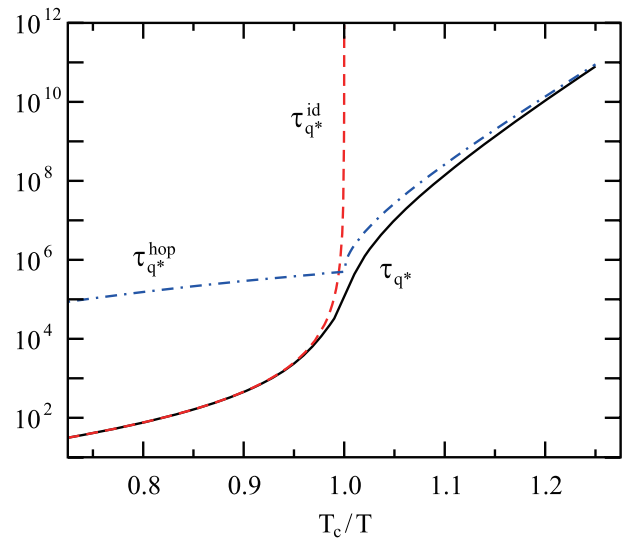


Figure 2. The α -relaxation time τ_{q^*} of the coherent density correlator at the structure factor peak $q^* = 7.3$ versus the inverse temperature T_c/T . The solid curve denotes the result from the extended MCT. The dashed curve refers to $\tau_{q^*}^{\text{id}}$ from the idealized MCT, which diverges at $T_c/T = 1$ with a power law $\tau_{q^*}^{\text{id}} \sim |T - T_c|^{-\gamma}$ [16]. The dashed-dotted curve represents $\tau_{q^*}^{\text{hop}}$ due to the hopping processes introduced in (7).

$T \leq T_c$ due to the presence of the hopping processes. One also infers from figure 1 that the hopping processes start to affect the density fluctuations at the temperature about 3% above T_c .

The α -relaxation time τ_{q^*} of the coherent density correlator at the structure factor peak $q^* = 7.3$ is plotted in figure 2 versus the inverse temperature T_c/T . Here the α -relaxation time is defined with the convention $\phi_q(\tau_{q^*}) = 0.1$. The dashed curve refers to $\tau_{q^*}^{\text{id}}$ from the idealized MCT, which diverges at $T_c/T = 1$ reflecting the mentioned bifurcation predicted by the idealized theory. Such a divergence is described by a power law $\tau_{q^*}^{\text{id}} \sim |T - T_c|^{-\gamma}$ [16]. The solid curve denotes the result from the extended MCT, in which the divergence predicted by the idealized theory is replaced by a smooth crossover.

The behavior of the α -relaxation time from the extended MCT can be understood on the basis of (7), according to which τ_{q^*} is determined by the smaller one of $\tau_{q^*}^{\text{hop}}$ and $\tau_{q^*}^{\text{id}}$. $\tau_{q^*}^{\text{hop}}$ from our model for the hopping kernel is included in figure 2 as the dashed-dotted curve. (We notice that f_q and f_q^s evaluated at $T = T_c$ enter (13) and (14) for $T \geq T_c$ since they determine the plateau height of the density correlators for this temperature regime [16], while T -dependent f_q and f_q^s enter the ones for $T < T_c$. This explains why $\tau_{q^*}^{\text{hop}} = i/\delta_{q^*}(z \rightarrow 0)$ from our model for the hopping kernel exhibits a square-root singularity near $T_c/T = 1$ [16].) One understands that τ_{q^*} agrees well with $\tau_{q^*}^{\text{id}}$ for $T_c/T < 1$ since $\tau_{q^*}^{\text{id}} < \tau_{q^*}^{\text{hop}}$ holds there, and the α -relaxation time in this temperature regime can be fitted well by a non-Arrhenius power law. On the other hand, τ_{q^*} crosses over to $\tau_{q^*}^{\text{hop}}$ for $T_c/T > 1$ since $\tau_{q^*}^{\text{id}} > \tau_{q^*}^{\text{hop}}$ holds there, and one infers from figure 2 that τ_{q^*} at low temperatures is nearly Arrhenius. Thus, the α -relaxation time predicted by the present theory exhibits the FSC at $T \approx T_c$.

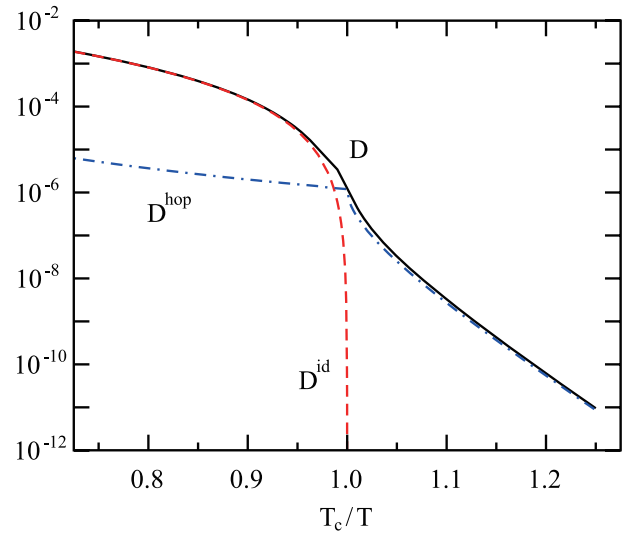


Figure 3. Self-diffusion constant D versus the inverse temperature T_c/T . The solid curve denotes the result from the extended MCT. The dashed curve refers to D^{id} from the idealized MCT, which vanishes at $T_c/T = 1$ with a power law $D^{\text{id}} \sim |T - T_c|^\gamma$ reflecting the dynamical arrest predicted by the idealized theory [16]. The dashed-dotted curve represents D^{hop} due to the hopping processes introduced in (12).

Figure 3 shows the corresponding result for the self-diffusion constant D : the solid curve denotes the result from the extended MCT; the dashed curve refers to D^{id} from the idealized MCT, which vanishes at $T_c/T = 1$ with a power law $D^{\text{id}} \sim |T - T_c|^\gamma$ reflecting the dynamical arrest predicted by the idealized theory [16]; and the dashed-dotted curve represents D^{hop} due to the hopping processes introduced

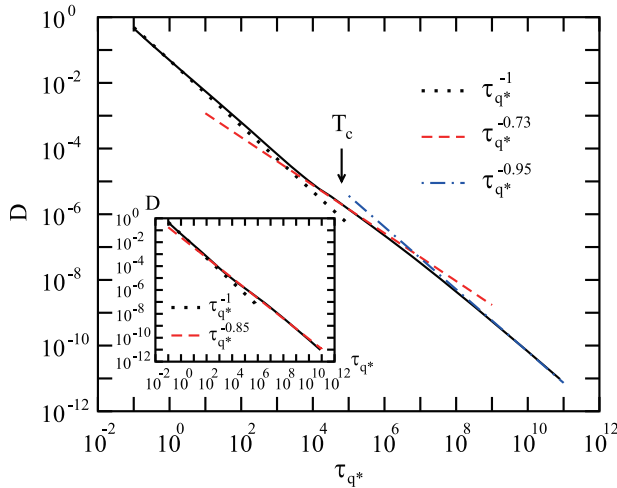


Figure 4. Double-logarithmic representation of the self-diffusion constant D versus the α -relaxation time τ_{q^*} of the coherent density correlator at the structure factor peak q^* (solid curve). The arrow indicates the location of T_c . The dotted line refers to the SER prediction $\sim \tau_{q^*}^{-1}$, while the dashed ($\sim \tau_{q^*}^{-0.73}$) and dashed-dotted ($\sim \tau_{q^*}^{-0.95}$) curves to fractional relations (see the text). Inset: D versus τ_{q^*} from the main panel (solid curve) is compared with the fractional relation $\sim \tau_{q^*}^{-0.85}$ (dashed curve).

in (12). Again, the behavior of D from the extended MCT can be understood on the basis of (12): D is determined by the larger one of D^{hop} and D^{id} , and this explains why D crosses over from $D \approx D^{\text{id}}$ to D^{hop} at $T_c/T \approx 1$. In addition, one infers from figure 3 that D exhibits nearly an Arrhenius behavior at low temperatures. Thus, the self-diffusion constant D predicted by the present theory also exhibits the FSC at $T \approx T_c$.

Let us now turn our attention to the Stokes–Einstein relation (SER) according to which the self-diffusion constant is inversely proportional to the α relaxation time, $D \sim \tau_{q^*}^{-1}$. (We confirmed that τ_{q^*} is proportional to the viscosity divided by the temperature, η/T , which can also be calculated from the extended MCT. The α -relaxation time τ_{q^*} is therefore used as a substitute for η/T in the present work.) The SER is known to be accurate for normal- and high-temperature liquids. The SER holds also within the idealized MCT since it predicts that both τ_{q^*} and $1/D$ exhibit a universal power-law behavior $|T - T_c|^{-\nu}$ for $T \rightarrow T_c+$ [16]. On the other hand, as already demonstrated in [15], the extended MCT predicts the breakdown of the SER near and below T_c which is in agreement with experimental observations in glass-forming liquids [23–25]. Here, we shall therefore focus on whether the SER breaks down in different ways on the fragile and strong sides of the FSC, motivated by such an observation in confined water [26].

The solid curve in figure 4 shows D versus τ_{q^*} in a log–log scale calculated from the extended MCT. It is seen that, while the SER holds at high temperatures (cf the dotted curve), the SER breaks down for temperatures near and below T_c . Such a violation of the SER is conventionally fitted by a fractional relation $D \sim \tau_{q^*}^{-x}$ with some exponent $0 < x < 1$. However, without any theoretical foundation, it is difficult to perform a physically meaningful nonlinear fit by the fractional relation.

In this regard, we notice a recent theoretical investigation of the SER violation which is based on two classes of kinetically constrained models, one describing diffusion in a fragile glass former and the other in a strong glass former [27]. The main result of [27] is that, while in the fragile case $D \sim \tau_{q^*}^{-0.73}$ which is weakly dependent on the dimensionality d , in the strong case the violation is sensitive to d , and $D \sim \tau_{q^*}^{-2/3}$ for $d = 1$ and $D \sim \tau_{q^*}^{-0.95}$ for $d = 3$.

It is seen from figure 4 that the fractional relations predicted by the kinetically constrained models (cf the dashed and dashed-dotted curves) fit our theoretical result well both in the fragile and strong regions. (Here we have used the exponent 0.95 for $d = 3$ in the strong region since it is appropriate for our LJ system.) Such an observation is in agreement with the experimental result for confined water in which the fractional relations with the exponents 0.73 and 2/3 are found to fit the data for the fragile and strong sides, respectively [26]. (Here the exponent 2/3 is appropriate for the strong side since water studied in [26] is confined in $d = 1$ cylindrical tubes.)

In the inset of figure 4, it is demonstrated that the violation of the SER in both the fragile and strong regions can be fitted reasonably well by a single fractional relation $D \sim \tau_{q^*}^{-0.85}$. However, since a theoretical foundation is lacking for the exponent 0.85, such a fit should be considered as an empirical one.

4. Concluding remarks

In this paper, it is argued that the extended MCT predicts a dynamic crossover in the α -relaxation time and in the self-diffusion constant as a general implication of the structure of its equations of motion. This crossover occurs near the critical temperature T_c of the idealized version of the theory and is caused by the change in the dynamics from the one determined by the cage effect to that dominated by hopping processes. When combined with the model for the hopping kernel developed in [15], the dynamic crossover can be identified as the FSC (see figures 2 and 3). Since our theory does not resort to the presence of the Widom line, to which the FSC in confined water is attributed [6, 7], it provides a possible explanation of the FSC observed in a variety of glass-forming systems [8–12]. Such an explanation based on the extended MCT seems reasonable since the crossover temperature $\approx 1.2T_g$ found in experiments is considered to coincide with T_c [10, 11].

The extended MCT also predicts that the SER breaks down in different ways on the fragile and strong sides of the FSC, in accord with the experimental observation in confined water [26]. This is illustrated in figure 4 in which the extended-MCT result is fitted with two fractional relations with exponents taken from kinetically constrained models for fragile and strong glass formers [27]. It is also demonstrated that the violation of the SER in both the fragile and strong regions can be fitted reasonably well by a single fractional relation with an empirical exponent 0.85 (see the inset of figure 4).

The results of the present work indicate the physical significance of the concept of T_c : it serves as the *crossover* temperature at which qualitative changes of behavior take place

in glass-forming systems. Besides the FSC, the breakdown of the SER also occurs near and below T_c as demonstrated in figure 4. In addition, many features of so-called dynamical heterogeneities set in at $T \approx T_c$ [15]. Furthermore, T_c can be considered as an onset temperature of the boson peak [20, 22]. In contrast, no singular characteristics from a physical point of view can be observed in the vicinity of the traditional glass transition temperature T_g .

Acknowledgments

This work was supported by Grant-in-Aids for scientific research from the Ministry of Education, Culture, Sports, Science and Technology of Japan (no. 20740245). Research at MIT is supported by DE-FG02-90ER45429.

References

- [1] Faraone A, Liu L, Mou C-Y, Yen C-W and Chen S-H 2004 *J. Chem. Phys.* **121** 10843
- [2] Liu L, Chen S-H, Faraone A, Yen C-W and Mou C-Y 2005 *Phys. Rev. Lett.* **95** 117802
- [3] Mallamace F, Broccio M, Corsaro C, Faraone A, Wanderlingh U, Liu L, Mou C-Y and Chen S-H 2006 *J. Chem. Phys.* **124** 161102
- [4] Poole P H, Sciortino F, Essmann U and Stanley H E 1992 *Nature* **360** 324
- [5] Debenedetti P G 2003 *J. Phys.: Condens. Matter* **15** R1669
- [6] Xu L, Kumar P, Buldyrev S V, Chen S-H, Poole P H, Sciortino F and Stanley H E 2005 *Proc. Natl Acad. Sci. USA* **102** 16558
- [7] Kumar P, Yan Z, Xu L, Mazza M G, Buldyrev S V, Chen S-H, Sastry S and Stanley H E 2006 *Phys. Rev. Lett.* **97** 177802
- [8] Laughlin W T and Uhlmann D R 1972 *J. Phys. Chem.* **76** 2317
- [9] Taborek P, Kleiman R N and Bishop D J 1986 *Phys. Rev. B* **34** 1835
- [10] Rössler E 1990 *J. Chem. Phys.* **92** 3725
- [11] Zöllmer V, Rätzke K and Faupel F 2003 *Phys. Rev. Lett.* **90** 195502
- [12] Faupel F, Frank W, Macht M-P, Mehrer H, Naundorf V, Rätzke K, Schober H R, Sharma S K and Teichler H 2003 *Rev. Mod. Phys.* **75** 237
- [13] Angell C A 1991 *J. Non-Cryst. Solids* **131–133** 13
- [14] Götze W and Sjögren L 1987 *Z. Phys. B* **65** 415
- [15] Chong S-H 2008 *Phys. Rev. E* **78** 041501
- [16] Götze W 1991 *Liquids, Freezing and Glass Transition* ed J-P Hansen, D Levesque and J Zinn-Justin (Amsterdam: North-Holland) p 287
- [17] Götze W and Sjögren L 1992 *Rep. Prog. Phys.* **55** 241
- [18] Hansen J-P and McDonald I R 1986 *Theory of Simple Liquids* 2nd edn (London: Academic)
- [19] Fuchs M, Götze W and Mayr M R 1998 *Phys. Rev. E* **58** 3384
- [20] Chong S-H 2006 *Phys. Rev. E* **74** 031205
- [21] Flynn C P 1968 *Phys. Rev.* **171** 682
Flynn C P 1972 *Point Defects and Diffusion* (Oxford: Clarendon)
- [22] Götze W and Mayr M R 2000 *Phys. Rev. E* **61** 587
- [23] Chang I and Sillescu H 1997 *J. Phys. Chem. B* **101** 8794
- [24] Swallen S F, Bonvallet P A, McMahon R J and Ediger M D 2003 *Phys. Rev. Lett.* **90** 015901
- [25] Mapes M K, Swallen S F and Ediger M D 2006 *J. Phys. Chem. B* **110** 507
- [26] Chen S-H, Mallamace F, Mou C-Y, Broccio M, Corsaro C, Faraone A and Liu L 2006 *Proc. Natl Acad. Sci. USA* **103** 12974
- [27] Jung Y J, Garrahan J P and Chandler D 2004 *Phys. Rev. E* **69** 061205